



# Consistency of the regional response to global warming levels from CMIP5 and CORDEX projections

Javier Diez-Sierra<sup>1</sup> · Maialen Iturbide<sup>1</sup> · Jesús Fernández<sup>1</sup> · José M. Gutiérrez<sup>1</sup> · Josipa Milovac<sup>1</sup> · Antonio S. Cofiño<sup>1</sup>

Received: 16 November 2022 / Accepted: 13 April 2023 / Published online: 25 April 2023  
© The Author(s) 2023

## Abstract

Assessing the regional responses to different Global Warming Levels (GWs; e.g. + 1.5, 2, 3 and 4 °C) is one of the most important challenges in climate change sciences since the Paris Agreement goal of keeping global temperature increase well below 2 °C with respect to the pre-industrial period. Regional responses to global warming were typically analyzed using global projections from Global Climate Models (GCMs) and, more recently, using higher resolution Regional Climate Models (RCMs) over limited regions. For instance, the IPCC AR6 WGI Atlas provides results of the regional response to different GWs for several climate variables from both GCMs and RCMs. These results are calculated under the assumption that the regional signal to global warming is consistent between the GCMs and the nested RCMs. In the present study we investigate the above assumption by evaluating the consistency of regional responses to global warming from global (CMIP5) and regional (CORDEX) projections. The dataset aggregated over the new IPCC reference regions, available from the IPCC AR6 WGI Atlas repository, is analyzed here for temperature and precipitation. The existing relationships between the regional climate change signals and global warming are compared for both CMIP5 and CORDEX. Our results show significant linear scaling relationships between regional changes and global warming for most of the regions. CORDEX and CMIP5 show remarkably similar scaling relationships and similar robustness in the emergence of the climate change signal for most of the regions. These results support the use of regional climate models in the context of global warming level studies.

**Keywords** Climate change · Global warming levels · Regional response · Regional climate models · CORDEX

## 1 Introduction

Global Warming Levels (GWs) provide a simple climate change dimension for assessing the regional responses of climatic variables and indices as a function of global warming (typically at + 1.5, 2, 3 and 4 °C levels). The use of GWs became widespread after the Paris Agreement goal of keeping global temperature increase well below 2 °C with respect to the pre-industrial period (UNFCCC 2016). As a result, many recent climate change impact and adaptation studies use GWs as a convenient and policy-relevant climate dimension (IPCC 2022), as an alternative to the use of fixed periods (typically near-, mid- and far-future) across different scenarios.

GWs are defined using Global Climate Model (GCM) projections to calculate mean climatic (e.g. 20-year averages) changes in Global Surface Air Temperature (GSAT) along the twenty-first century, relative to a pre-industrial period, typically 1850–1900 (Seneviratne et al. 2021; Cross-Chapter Box 11.1). For a particular warming level (e.g. + 2 °C), the periods when each model first reaches this warming threshold are annotated (different periods for different models) and then used to compute the corresponding regional changes as differences between the variable values in these periods and the baseline. There seems to be a consensus on the fact that GWL responses are consistent across different scenarios for many climate variables (Pendergrass et al. 2015; Seneviratne et al. 2016; Seneviratne and Hauser 2020; Wartenburger et al. 2017), even though there are studies showing small but significant dependencies of the scaling pattern on emission scenarios, especially at middle and high latitudes of the Northern Hemisphere (Maule et al. 2017; Ishizaki et al. 2012). Therefore, it is common practice to

✉ Javier Diez-Sierra  
javier.diez@unican.es

<sup>1</sup> Instituto de Física de Cantabria (IFCA), CSIC-Universidad de Cantabria, Santander, Spain

pool across models and scenarios the regional change signals for each particular level. GWL information is typically displayed in the form of maps representing the spatial change patterns of variables or indices for specific GWLs (see e.g. Gutiérrez et al. 2021) or as regional climate sensitivity plots, displaying changes of the regionally aggregated variable of interest versus the global warming level (Seneviratne and Hauser 2020). The latter can be expressed as the rate of change of a variable over a region (e.g. degrees change of temperature or percent change of precipitation) per degree increase in GSAT. This approach implies a linear relationship between patterns of regional climate change and the average global temperature change, which was already found for several variables in Europe (Matte et al. 2019).

GWL products are typically obtained using multi-model ensembles of centennial global climate projections produced in the Coupled Model Intercomparison Project (CMIP). The two latest ensembles available are CMIP5 (Taylor et al. 2011) and CMIP6 (Eyring et al. 2016), with typical GCM resolutions of around 200 and 100 km, respectively. Moreover, GWLs have been extended to work also with Regional Climate Models (RCMs). RCMs provide higher resolution results operating over a limited region as compared to the GCM outputs that drive them at the boundaries (Gutowski et al. 2020; Jacob et al. 2020; Giorgi et al. 2022). In particular, the Coordinated Regional Climate Downscaling Experiment (CORDEX, <https://cordex.org>) provides multi-model ensembles of regional climate projections driven by CMIP5 model outputs over 14 continental domains for a variety of GCM and RCM combinations (Giorgi and Gutowski 2015; Gutowski et al., 2016). These regional projections are highly demanded for regional impact and adaptation studies and their resolution ranges from 50 to 10 km, depending on the domain. GWLs have been extensively used in the latest IPCC report to assess regional climate change (IPCC 2021a). In particular, the Atlas Chapter and the Interactive Atlas (Gutiérrez et al. 2021) provide GWL results for both global CMIP5 and CMIP6 and regional CORDEX multi-model ensembles, facilitating the analysis of regional climate sensitivity to global warming for global and regional climate simulations.

The main problem to extend the GWL methodology to RCMs is that they operate on regional domains and, therefore, they do not provide global GSAT information to compute the periods when GWLs are reached. To overcome this problem, the standard practice has been to use the corresponding periods from the driving GCM as a proxy (Déqué et al. 2017; Nikulin et al. 2018; Ciarlo et al. 2021), under the assumption that these proxy periods are suitable for estimating the regional climate sensitivity of RCMs as a function of global warming. Assessing the consistency of regional climate change sensitivity between RCM simulations and their driving GCMs across broad climatic regions

would shed some light on this assumption and is key for further research exploring the added value of regional vs global projections for regional GWL studies.

Here, we explore this problem by analyzing the consistency between CMIP5 and CORDEX for different GWLs, using the data available from the IPCC-WGI Atlas repository (Iturbide et al. 2021, 2022) over the IPCC AR6 reference regions (Iturbide et al. 2020). In particular, we analyze the regional responses to global warming using GWL scaling plots (Seneviratne and Hauser 2020). These plots represent regionally aggregated changes (for mean temperature and precipitation in this work) vs GSAT changes for successive decadal periods along the twenty-first century. We investigate the existence of significant linear relationships (scaling) supporting the use of GWLs as an informative climate dimension in these cases (e.g. using the amount of regional change per unit of global warming, e.g. per degree of warming). Moreover, we analyze the influence of the emission scenario in the results. And finally, we analyze the robustness of the regional response, calculated for every decade of the twenty-first century, annotating the mean GWL where the regional climate change signal emerges consistently from natural model variability. Here, we combine the GWL plots with the robustness approach defined in the IPCC (Gutiérrez et al. 2021; Cross-ChapterBoxAtlas.1). The goal is assessing the consistency of CMIP and CORDEX by comparing the results of both approaches (scaling relationships and the robustness in the emergence of the climate change signal) in the reference regions.

The paper is organized as follows. Section 2 presents the data and methods used. Results are described in Sec. 3. Finally, Sect. 4 provides the main conclusions of this work.

## 2 Data and methods

### 2.1 CORDEX and CMIP5 regionally-aggregated datasets

We use the regionally aggregated dataset available from the IPCC-WGI Atlas repository for CMIP5 and CORDEX simulations (Iturbide et al. 2021, 2022). This dataset contains monthly means of temperature and precipitation spatially averaged over the IPCC AR6 reference regions (Iturbide et al. 2020), which represent subcontinental climatologically consistent areas. Results are available for land, sea and land-sea grid boxes separately. For the present analysis, we consider the results aggregated over all grid boxes (land-sea dataset) for the historical experiment and the RCP8.5 scenario. The RCP8.5 scenario is chosen because 1) it allows exploring higher GWLs (e.g. 4 °C) and 2) this is the scenario with the highest number of simulations available,

thus reducing the uncertainty related to small ensemble sizes (Dosio et al. 2019).

The Atlas repository provides aggregated information for CMIP5 (28 GCMs, including those used to drive all CORDEX simulations) and CORDEX (33 RCMs, considering all different configurations and versions). For the latter, the dataset includes 11 out of the total of 14 official CORDEX domains covering almost entirely the continental regions of the world with a large number of simulations (Diez-Sierra et al. 2022). The number of available RCMs varies for each CORDEX domain resulting in different ensemble sizes, being Europe the domain with the highest number of RCMs (12) and the Antarctic domain with the lowest (3). The simulations available for each CORDEX domain are accessible through the IPCC WGI AR6 Annex II (IPCC 2021b: Annex II) and the IPCC-Atlas repository (Iturbide et al. 2021, 2022). Following the methodology applied in the IPCC-WGI Atlas (Gutiérrez et al. 2021), the mosaic ensemble approach is used to build a world-wide CORDEX dataset by selecting the CORDEX domain that best fits each AR6 reference region (Diez-Sierra et al. 2022, see their Fig. 1b).

Here, we analyze the results for 42 out of the total of 46 land reference regions. Four Asian regions (EEU, WSB, ESB and RFE, grayed out in Fig. 4) were discarded since the CORDEX domains used in the work do not properly cover them (less than 80% overlap). The Arctic region (ARO) was the only oceanic region included in the analysis. For each region we used the corresponding set of CORDEX RCM

simulations and the subset of CMIP5 GCMs driving them. The latter were weighted according to the frequency each GCM was used as boundary conditions in the corresponding CORDEX domain, following Boé et al., (2020). This means that, if one specific GCM drives e.g. two different RCMs, then this GCM will weigh twice in the analysis (i.e. to calculate the slope and the robustness). Despite this weighting, note that there are typically several RCMs driven by the same GCM, which tends to enlarge the uncertainty of the CORDEX ensemble with respect to the CMIP5 one.

## 2.2 Regional responses to global warming: GWL plots

In order to analyze the regional responses of mean temperature and precipitation to different GWLs, we use *regional climate sensitivity plots* (Seneviratne and Hauser 2020), which are called GWL scaling plots in the IPCC Interactive Atlas (Gutiérrez et al. 2021; <http://interactive-atlas.ipcc.ch>). The latter are computed in a slightly different way to avoid the redundant information arising from running means that can overlap for different GWLs. Namely, for a given climate variable or derived climate index and a region of interest, the GWL plot is a scatter plot representing the regionally aggregated changes vs the GWL; each point in the plot represents both magnitudes for a particular period (e.g. 10-years) along the twenty-first century. GWLs and regional changes are typically computed using the pre-industrial baseline period 1850–1900.

CORDEX historical simulations do not cover the pre-industrial baseline period and, therefore, an alternative baseline corresponding to modern climate is used in some cases for calculating regional changes. In this study we use the AR5 1986–2005 reference modern period to calculate regional changes, and the pre-industrial baseline period 1850–1900 to calculate the GSAT increase with CMIP5. This modern reference period approach can also be selected in the IPCC Interactive Atlas to compute GWL plots for all available indices for CMIP5 and 6. As an illustrative example, Fig. 1 shows a GWL plot generated by the Interactive Atlas for the Mediterranean (MED) precipitation from CMIP5. The points represent individual model values calculated for every decade of the twenty-first century. On the x-axis, this plot displays the global warming levels computed as changes of CMIP5 mean GSAT relative to the 1850–1900 pre-industrial baseline period, from +0 to +6 °C. On the y-axis, regional (MED region) relative changes computed as relative regional changes of precipitation, relative to the 1986–2005 baseline, are displayed. Note that different baselines can be selected in the Interactive Atlas. In these figures, global warming values are calculated using a total of 28 CMIP5 model projections. Every point corresponds to future

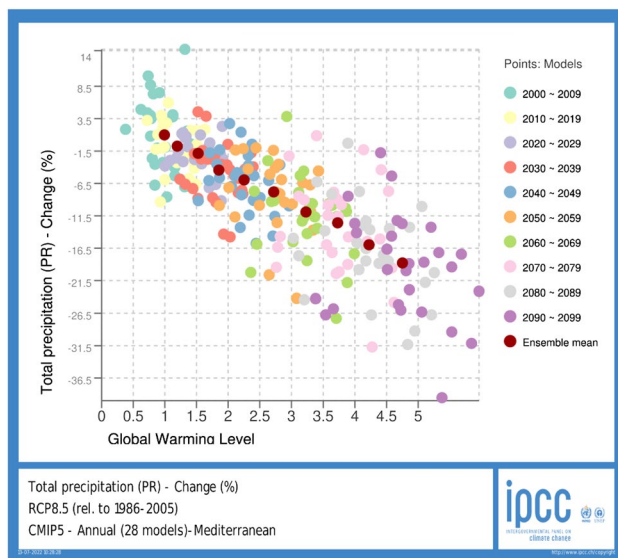


**Fig. 1** Regional precipitation responses to global warming for the Mediterranean region obtained from CMIP5 for the RCP8.5 scenario. The period 1986–2005 is selected as the baseline to compute the regional changes for the twenty-first century. The Mediterranean region is shown in Fig. 4. Source: IPCC WGI AR6 Interactive Atlas (Gutiérrez et al. 2021)

change values for every model and decade of the twenty-first century (280 points), with different decades in different colors. Red points show the decadal ensemble means.

In the Supplementary Material (Fig. S1), we compare this approach to the location of time periods corresponding to preset GWL values on the x-axis, which are then used to compute the regional average response for that particular period (y-axis). Results are qualitatively very similar and are based on the same background information. However, the decadal means shown in this study and in the Interactive Atlas represent independent samples of the regional response to global warming, while the running mean approach produces redundant information arising from overlapping running windows and also drops valuable information from simulations not reaching high GWLs (see also Fig. SM2).

### 2.3 Linear scaling and robustness of regional responses

Building on the GWL plots described in the previous section, we investigate the existence of significant linear relationships between the regional climate signals and the GWL across variables and regions. For that, we perform a significance test against the null hypothesis that the linear slope of the corresponding GWL plot is zero, using a Wald t-test with a 99% confidence ( $p$ -value below 0.01). Significant relationships indicate scaling of the regional climate change signal with global warming and supports the use of GWLs as an informative climate dimension in these cases (e.g. using the amount of regional change per unit of global warming, e.g. per degree of warming).

These significant scaling relationships are typically found for variables and regions with robust climate change signals (Sect. 3). Therefore, we also calculate the robustness of the regional signals along the decades of the twenty-first century, building on the GWL plot. For each decade, we compute the robustness of the multi-model mean signal using the advanced approach defined in IPCC-WGI AR6 (Gutiérrez et al. 2021, Cross-ChapterBoxAtlas.1). This methodology uses the individual GCM signals to classify the multi-model mean signal into three categories: (1) robust signal, (2) conflicting signal, and (3) no change or no robust signal. Categories 1 and 2 correspond to ensembles with a likely robust signal, characterized by over 2/3 of the models exhibiting robust signals (see below). Model agreement on the sign of change leads then to a robust (category 1) or conflicting (category 2) signal. Category 3 indicates no change (signal close to zero) or no robust change (less than 1/3 of the models exhibiting robust signals). Robust model signals are interpreted as (decadal) signals emerging from natural (decadal) variability. In practice, this is computed using a threshold  $\gamma = 1.645\sqrt{2/10}\sigma_{1\text{yr}}$ , corresponding to a 90% confidence interval for decadal interannual variability, where

$\sigma_{1\text{yr}}$  is the interannual standard deviation computed from the linearly detrended baseline period 1970–2005 (which is used as an approximation when a long historical period is not available, as in CORDEX). For consistency, and following Gutiérrez et al. 2021 (Cross-ChapterBoxAtlas.1), we use the same period to calculate the threshold  $\gamma$  for CORDEX and CMIP5 historical simulations.

In this work, the GWL plot used in the Interactive Atlas (Fig. 1) is expanded by annotating robustness information for the ensemble mean decadal results, indicating with different symbols the above-mentioned categories for robustness. This allows estimating the mean GWL value for which the regional signal emerges consistently from natural model variability. This is inspired in the concept of temperature of emergence (ToE), defined in previous studies by applying different methodologies to estimate the threshold under which the climate change signal emerges consistently from natural variability (Kirchmeier-Young et al. 2019; Seneviratne and Hauser 2020). Here, we perform a gross estimation of the ToE (defined here as mean GWL emergence) by combining the GWL plots with the robustness approach defined in the IPCC (Gutiérrez et al. 2021, Cross-ChapterBoxAtlas.1; Doblas-Reyes et al. 2021, Sec. 10.4.3.2). Note that, for the sake of comparison between CORDEX and CMIP5, the robustness information calculated in this work are based on regional changes relative to a modern period, and therefore the results are offset as compared to a pre-industrial baseline.

## 3 Results

We compare the results of the regional response to global warming from CMIP5 and CORDEX for every reference region, variable (temperature and precipitation) and season. GWL plots are used to visualize and test the existence of a linear scaling of the regional response to global warming and to display the robustness of the multi-model decadal regional change signals along the twenty-first century, estimating the mean GWL emergence as defined in Sect. 2.

As an example, we first analyze the GWL plots for two different regions with significant regional signals and responses to global warming (Figs. 2 and 3, corresponding to temperature in the Arctic and precipitation in the Mediterranean, respectively). These figures are illustrative examples of the analysis carried out over the 43 reference regions, for both temperature and precipitation, and for annual and seasonal (DJF, MAM, JJA and SON) temporal aggregations for the regional responses. Note that GWLs are always computed from annual GSAT values.

Figure 2 shows the regional climate response in the Arctic Ocean (ARO) region. Black open dots on the left two panels of the figure correspond to CMIP5 models which did not drive any CORDEX model for this region. These models



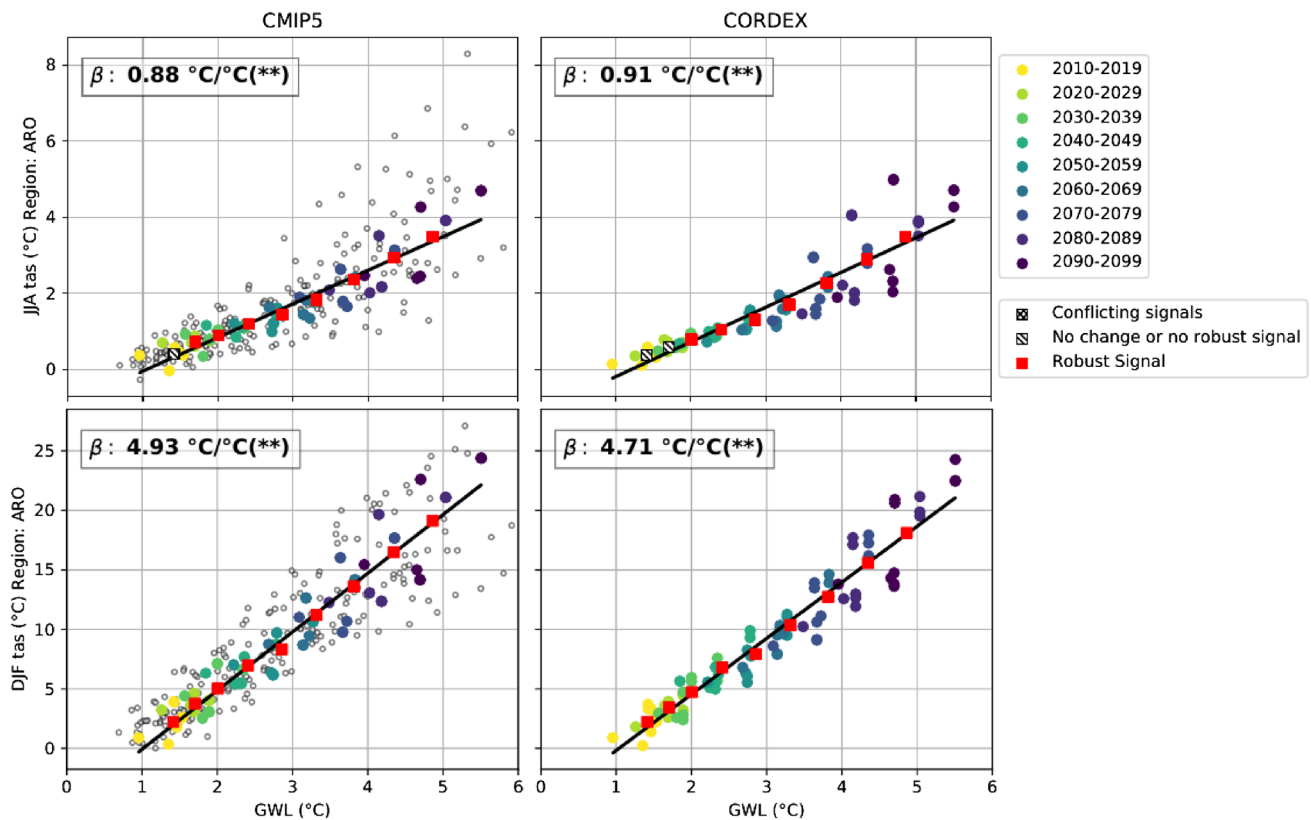


**Fig. 2** GWL plots displaying regional air temperature responses to global warming over the Arctic Ocean (ARO) for CMIP (left) and CORDEX (right). Top- and bottom-side panels show the regional response for summer (JJA) and winter (DJF), respectively. Coloured points represent model changes (regional changes vs global warming values) for every decade of the twenty-first century with respect to the baseline; note that different baselines are used for calculating the GWLs (1850–1900) and regional response (1986–2005). Black open dots in the left column indicate results for CMIP5 models which do not drive any CORDEX model for this particular region.  $\beta$  denotes

the slope of the linear fit (black line) using all available projections or points (except for the black open dots). The asterisks indicate the significance of the slope –two asterisks (\*\*) for  $p \leq 0.01$ , one asterisk (\*) for  $0.01 < p \leq 0.05$  and no asterisks for  $p > 0.05$ . Squares represent the decadal ensemble mean values and robustness (red, hatched or crossed-out squares) for every decade of the twenty-first century. Note that regional changes (y-axis) are relative to a modern reference and therefore are offset as compared to a pre-industrial baseline

are not used in the analysis and are only included in the plot to show the dispersion of the entire CMIP5 GCM ensemble, as compared to the GCM selection used to drive CORDEX RCMs (in colors, according to the decade; see legend). Squares represent, for every decade of the twenty-first century, the ensemble mean decadal results and robustness (see legend). As can be seen in Fig. 2, there is a significant relationship ( $p$ -value  $< 0.01$ , represented by the asterisks in the slope value) between regional temperature changes and GWL. This is true for both CMIP5 and CORDEX (in columns) and for both seasons (in rows), with a very high regional response in winter (DJF), when there is a regional to global warming factor above 4.5. Similar values of the slopes are obtained for CMIP5 and CORDEX, indicating high consistency between both global and regional projections. Regional climate signals are robust (decadal means in red) for all decades in winter, indicating that the climate

change signal has already emerged in these model ensembles. In summer, all decades except for the first one(s) are also robust, indicating a mean GWL emergence around  $1.5^\circ$  for CMIP5 and  $2^\circ$  for CORDEX. Note that the first decades are very close to the baseline periods used to compute the climate changes (1986–2005) and to determine the threshold for the robustness analysis (1970–2005). Therefore, the results for these first decades are susceptible to being affected by the internal variability of the models.

Figure 3 shows the regional climate responses of precipitation change in the Mediterranean (MED) region. The decreasing trends are significant in all cases with summer (JJA) changes around  $-10\%$  per  $^\circ\text{C}$  for CMIP5 and  $-8\%$  per  $^\circ\text{C}$  for CORDEX. Winter (DJF) trends are around  $-3\%$  per  $^\circ\text{C}$  for both ensembles. Figure 3 allows distinguishing those CORDEX simulations driven by the same GCM, since they share the same GWL value on the x-axis and, therefore, they

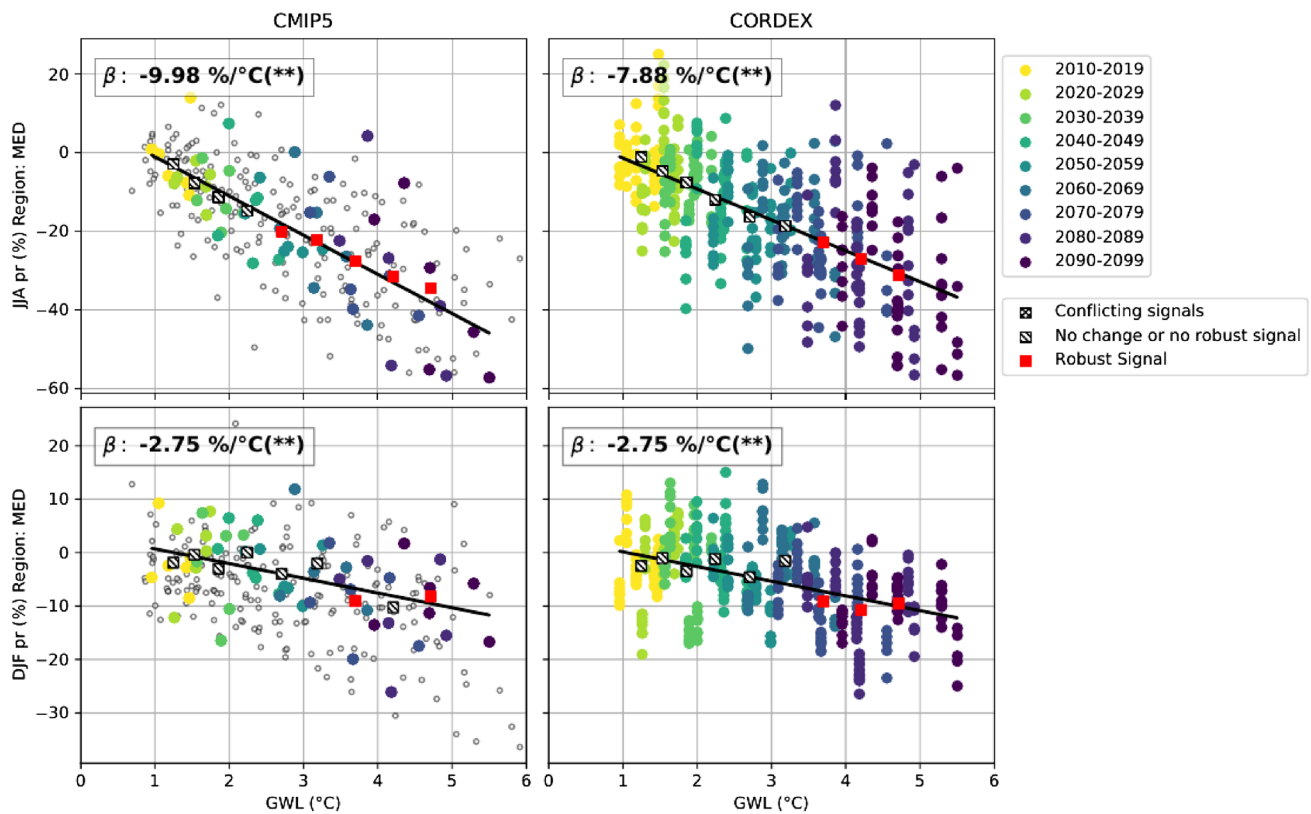


**Fig. 3** As Fig. 2, but for regional precipitation responses (relative change, as %) to global warming for the MED region

are spread only vertically. Robustness is also similar in winter with a mean GWL emergence around 3.5°C (although CMIP5 results show an interrupted emergence signal), but slightly different for summer, with a GWL emergence between 2.5 and 3.5 degrees, according to CMIP5 and CORDEX, respectively.

Up to now we have assumed that the emission scenario does not influence the regional response to global warming. To test this hypothesis, we compare the regional scaling response (i.e. the slopes  $\beta$  in Figs. 2 and 3) for the different IPCC reference regions for the RCP4.5 and RCP8.5 scenarios. Figure 4 assesses the impact of the emission scenario in the regional scaling responses for temperature (top four panels) and precipitation (bottom four panels). Regional scaling responses, and their differences between CMIP5 and CORDEX, are also shown to compare both sources of uncertainty. Upper left panels show the slope of the reference regions for CORDEX. Upper right panels show the slope differences between CMIP5 and CORDEX. Bottom panels show the slope differences between the scenarios RCP8.5 and RCP4.5 for CMIP5 (bottom-left) and CORDEX (bottom-right). For the bottom panels (scenario assessment) only the simulations available from both scenarios were selected. Moreover, the slopes were calculated with a limit GWL of 3 °C, which is approximately the maximum GWL reached for

RCP4.5. Otherwise, using all the information available for the XXI century, the slopes for the different scenarios can easily show significant differences due to the different sampling uncertainty. Only those regions with significant linear scaling to the 0.01 level were displayed; hatching indicates non-significant slopes in the upper left panels.

Figure 4 shows, in general, small differences between the scenarios RCP8.5 and RCP4.5. The differences are of the same order of magnitude as the differences between CMIP5 and CORDEX. For temperature, the average relative difference between global and regional models is around 5%, while the relative difference between scenarios varies from 4 to 6% for CMIP5 and CORDEX. The largest relative differences between scenarios take place in North America, northern Russia and Antarctica ( $\sim 0.3$  °C/°C). However, the small sample size for the Antarctic CORDEX domain might affect the results in this region. For precipitation, the average difference between projects is around 0.7%, while the difference between scenarios varies from 1.2% to 0.7% for CMIP5 and CORDEX. The largest differences between scenarios take place in Greenland and India for CMIP5 ( $\sim 3\%$ °C).

Figure 4 highlights the impact of the ensemble size in the results. The small number of simulations available for both scenarios translates into poor ensemble sizes for some of the domains. This leads to non-significant linear scaling for

most regions for precipitation, for which only 11–14 regions show significant linear scaling relationships in the scenario assessment.

For an exhaustive assessment of the consistency of the scaling results obtained for CMIP5 and CORDEX, we use heat maps (Fig. 5) summarizing the regional scaling (i.e. the slopes  $\beta$  in Figs. 2–3) for the different IPCC reference regions (in rows) and for all seasons (in columns). Regions are sorted according to the magnitude of CMIP5 global warming, with higher values at the top of the figure. In order to facilitate the comparison of the results, each cell is divided in two, representing the results for CMIP5 in the upper triangle and for CORDEX in the lower triangle. As in the annual case (Fig. 4), CMIP5 and CORDEX slopes are remarkably similar for most of the regions and for both variables.

The scaling relationships show high variability across seasons, particularly for precipitation, with significant slopes found typically for particular seasons (hatching in Fig. 5 indicates non-significant slopes). Temperature trends are significant with 99% confidence for the entire subset of regions and seasons analyzed. Regions located in high latitudes of the North hemisphere (ARO, RAR, NEN, NWN and GIC; in rows 1–5) show remarkably higher slopes for temperature in the Boreal winter (DJF) than in the rest of the seasons. Contrarily, Antarctic regions (WAS and EAN, rows 20 and 27) experience the highest regional response in the Boreal summer. The ARO region (row 1) experiences the highest regional warming as well as the highest relative increase in precipitation. The Arctic Amplification, produced by local positive feedbacks (e.g. temperature and surface albedo feedbacks, among others), plays an important role in the region (Liang et al. 2022). Finally, regions with a high percentage of ocean areas (SCA, SWS, NAU, SEA, MDG, CAR, SAU, NZ and SSA, on rows 35–43) present slopes lower than 1 for temperature, which just confirm the milder increase in temperature over oceanic regions as compared to the continental ones.

For temperature, the largest differences ( $0.3^\circ$ ) between CORDEX and CMIP5 are found in the Arctic Ocean (ARO, on row 1), Russian Arctic (RAR, on row 2), East Central Asia (ECA, on row 6) and Western and Central Europe (WCE, on row 18). The former two (ARO and RAR) are regions with high signal and thus smaller relative differences than in other regions. Regions with seasonal snow cover, such as ECA (row 6), show higher inconsistencies between CMIP5 and CORDEX. Seasonal snow cover is handled by the land surface model and is likely to differ between the RCM and the driving GCM; this deserves further investigation since other discrepancies, such as aerosol treatment, could also play a significant role.

Precipitation shows higher variability than temperature. However, most of the regions show high consistency

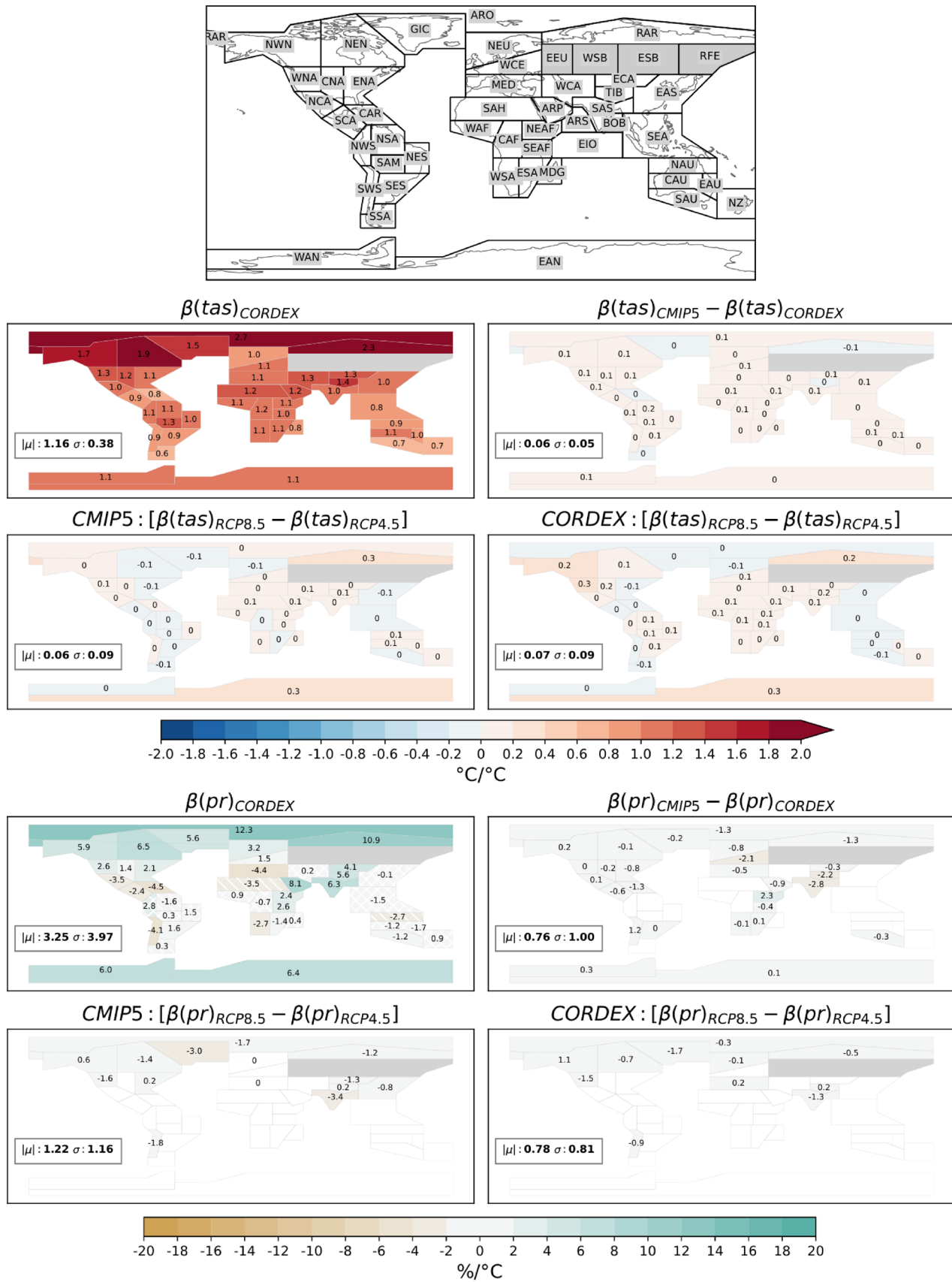
between CMIP5 and CORDEX. The largest inconsistencies are found in dry regions (e.g. Sahara region, SAH, on row 14), where small changes in precipitation lead to great relative changes. In addition, the driving GCMs usually exhibit large biases over dry regions, which are generally reduced by the RCM simulations (Teichmann et al. 2021). Regions with no significant trends tend to show lower values of slopes  $\beta$  and less consistency between CMIP5 and CORDEX. North and central South America regions (SAM, NSA and NES, in rows 7, 10 and 30) exhibit one of the major deviations between CMIP5 and CORDEX.

Figure 6 shows the mean GWL emergence for both CMIP5 and CORDEX. Darker colors indicate regional climate signals emerging for lower GSAT values, with white cells indicating that the regional climate signal does not emerge consistently during the twenty-first century using the RCP8.5 scenario. Overall, Fig. 6 shows similar values of GWL emergence for temperature and precipitation for CMIP5 and CORDEX. It is important to highlight that all the cells which reach a value of GWL emergence (non-white cells) exhibit significant linear GWL scaling relationships, which demonstrate the consistency of both approaches.

For temperature, the inconsistencies found in Fig. 5 do not hold in Fig. 6 for most of the cases. Note that for temperature, CMIP5 and CORDEX reach the mean GWL emergence during the first decades (low GWL) of the twenty-first century, even for those regions where the slope between CMIP5 and CORDEX is different. Western and Central European and Western Antarctic regions (WCE and WAN, in rows 18 and 20) exhibit the largest discrepancies for winter (DJF). However, in both cases, these discrepancies seem to be due to the internal variability of the models that may play an important role in the first decades of the twenty-first century; in fact, the slope  $\beta$  is consistent in both cases (see Fig. 5).

Precipitation shows higher variability than temperature; however, the results of GWL emergence are still remarkably similar for both datasets. Some discrepancies are also found for some regions with seasonal snow cover (Russian Arctic and Greenland/Iceland; RAR and GIC, rows 2 and 5). East Central Asia, Northern South America and East Asia regions (ECA, NSA and EAS, on rows 6, 10 and 22) also show some inconsistencies between CMIP5 and CORDEX for some of the seasons. Tibetan Plateau and North-Western South America regions (TIB and NWS, on rows 8 and 23) show the highest discrepancies for summer (JJA) and winter (DJF) seasons, respectively.

There are some reasons that can be identified to cause the discrepancies found between CMIP5 and CORDEX. It is well known that the change in resolution and improved representation of land surface characteristics significantly affects the representation of the local processes and the feedbacks (land–atmosphere, land–ice, sea–ice, ice–albedo), which might have an impact at regional scale (Goosse et al.





**Fig. 4** Regional scaling response for the different IPCC reference regions for temperature (top four panels) and precipitation (bottom four panels). Regions with significant linear scaling to the 0.01 level were displayed (hatching indicates non-significant slopes in the upper left panels). Upper left panels show the slope of the reference regions for CORDEX. Upper right panels show the slope differences between CMIP5 and CORDEX. Bottom panels show the slope differences between the scenarios RCP8.5 and RCP4.5 for CMIP5 (bottom-left) and CORDEX (bottom-right). For the bottom panels (scenario assessment) only the simulations available for both scenarios were selected. Slopes were calculated with a limit GWL of 3 °C

2018; Hohenegger et al. 2009; Iles et al. 2020; Müller et al. 2021; Seneviratne et al. 2006). In addition, several studies agree with the major deviations found here. For the Western and Central European region (WCE, on row 18), for example, CMIP5 is known to project a higher increase in temperature changes than CORDEX for summer, mainly caused by GCM/RCM differences in aerosols representation and atmospheric physics (Boé et al. 2020; Taranu et al. 2022). This also affects evapotranspiration, with likely impact clouds and precipitation, and thus explaining the differences shown in Fig. 5. Another example is the investigation carried out by Falco et al. (2019) in South America. They demonstrate the added value of the RCMs in reproducing the summer climatology for different South American regions situated in tropical and subtropical latitudes. Their results are aligned with the deviations found here for precipitation for South America Monsoon, Northern South America and North-Eastern South America regions (SAM, NSA and NES; in rows 7, 10 and 30; see Fig. 5).

In the supplementary material (Fig. SM3), we show the ToE calculated with the usual approach (see SM for more details). Results are qualitatively very similar for both approaches, however, the decadal means shown in this study can be interpreted as a gross estimation of the ToE shown in Fig. SM3. Note that the ToE is independent of time.

## 4 Conclusions

We analyzed the consistency of the regional response to global warming between CORDEX and CMIP5 projections. Regional climate change signals for temperature and precipitation as a function of global surface air temperature (GSAT) change were studied for 43 out of 61 reference regions used in the IPCC-WGI AR6, including most of the land regions plus the Arctic Ocean. Furthermore, we assess the influence of the emission scenarios in the results. The results were represented in the form of GWL plots, and their slopes and mean GWL values for which the regional signal emerges consistently were summarized for all regions and seasons.

Our results demonstrate high consistency in the regional response to global warming between global and regional

climate projections. CORDEX and CMIP5 datasets show remarkably similar regional scaling relationships with respect to the global warming level for most regions analyzed. For temperature, significant and positive linear trends are found between the regional response and global warming for all regions and seasons analyzed. For precipitation, most regions show significant linear trends in at least one of the seasons. The analysis of robustness reveals similar GWL values for which regional signal emerges consistently between CORDEX and CMIP5. Robust signals were found for all the regions and seasons for temperature after the first decades, which indicates that the GWL emergence has already been exceeded for all the cases. For precipitation, similar GWL emergence values were also found for both datasets, although for some of the regions analyzed the robust climate signal emerged intermittently and therefore the temperature of emergence is not reached in these cases. Those regions in which the robustness analysis emerges consistently also show significant linear scaling relationships between the regional response and global warming; thus indicating that both analyses are consistent.

Regions with large seasonal snow covered areas, mostly located in the Russian Arctic and in North America, show some inconsistencies for the winter months for CORDEX and CMIP5. The largest inconsistencies for precipitation are found in dry regions (e.g. Sahara region) since in these regions small changes of precipitation often lead to great relative changes. Although, overall, we showed the high consistency between CMIP5 and CORDEX, it is key to identify the reasons behind the different response of GCMs and RCMs for some of the regions. For example, Taranu et al. (2022) demonstrate that wrong selection in GCM/RCM pairs (i.e. different configuration in aerosols and atmospheric physics) can explain the inconsistencies found for the Western and Central European region. The lack of plant physiological response to increased CO<sub>2</sub> levels in many RCMs has also been identified as a key source of discrepancy over central and northern Europe (Schwingshackl et al. 2019), but these kind of analyses need to be extended to the rest of the regions identified in this study (i.e. regions in which the GCMs and RCMs climate signals differ) in order to understand the mechanisms behind these discrepancies and discern between genuine added value and inconsistent model setup.

Our results show that the influence of the emission scenario (RCP4.5 or RCP8.5) is low, and of the same order of magnitude as the influence of the project (CMIP5 or CORDEX). For temperature, the average relative difference between regional and global models is around 5%, while the difference between scenarios varies from 4% (CMIP5) to 6% (CORDEX). For precipitation, the average difference between regional and global models is around 0.7%,

**Fig. 5** Heat map for the slope of the regional temperature (left panel, units: °C/°C) and precipitation (right panel, units: %/°C) change with respect to the GWL. Cells division represents the results for CMIP5 (top triangle) and CORDEX (bottom triangle). Different seasons are shown in columns and IPCC reference regions are in rows. Simple hatching hides non-significant slopes to the 0.01 level (double hatching for those not significant to the 0.05 level)

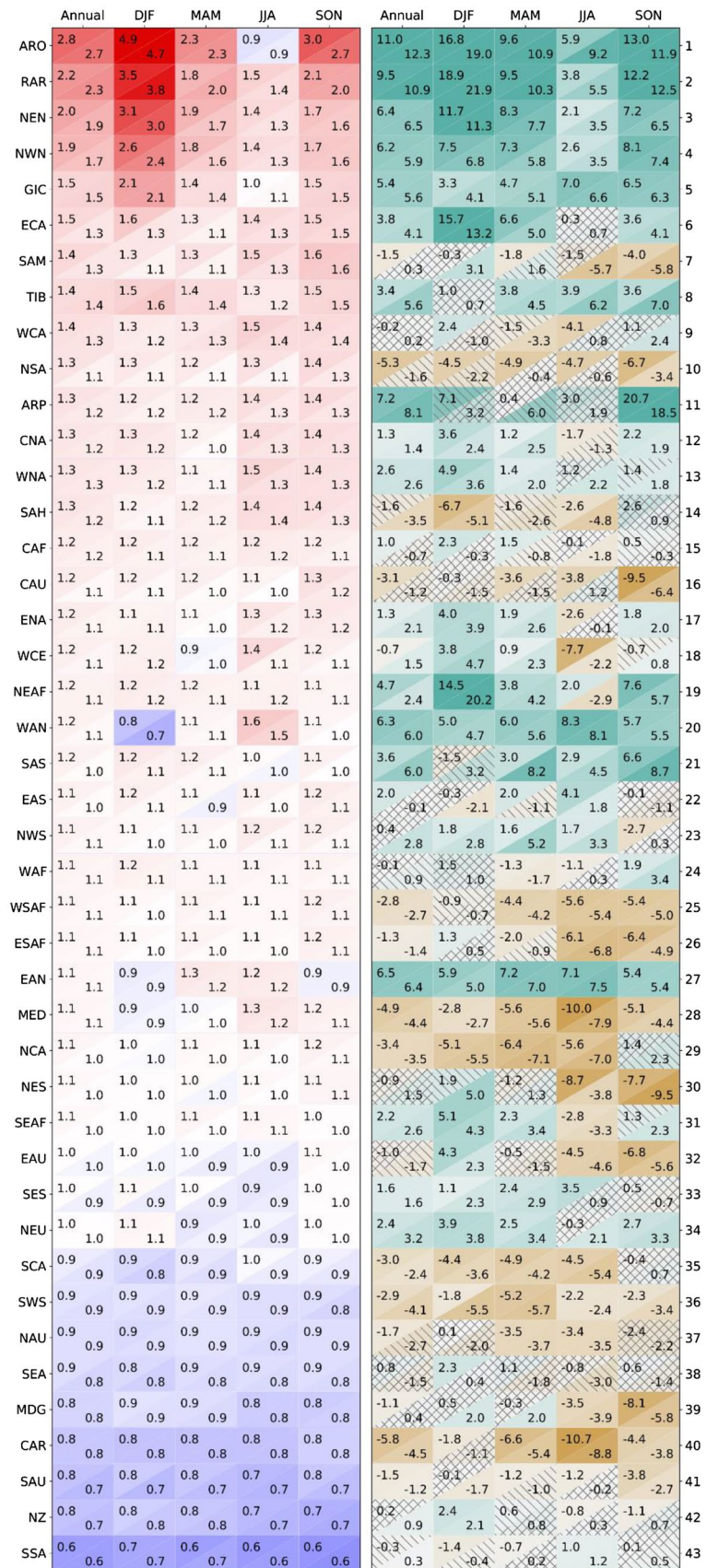
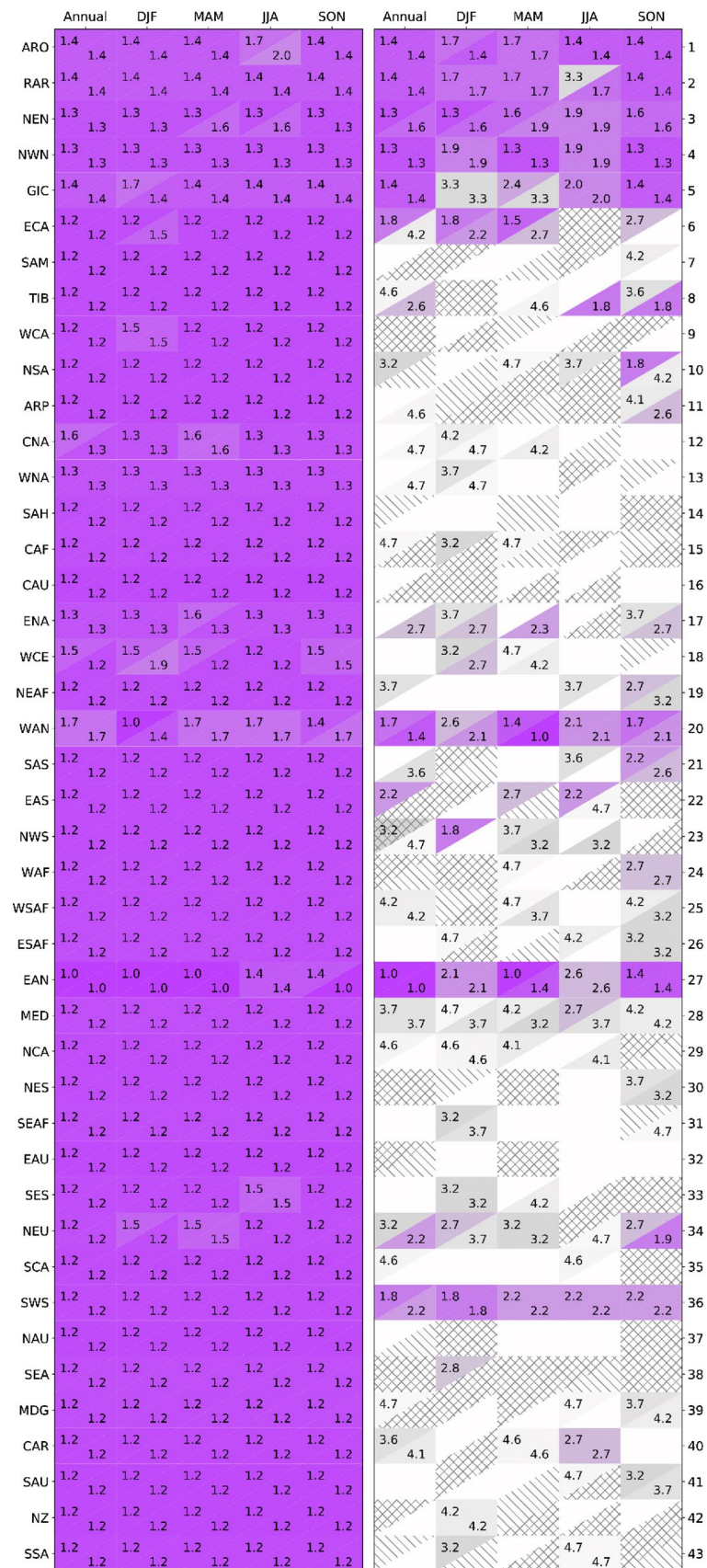




**Fig. 6** As Fig. 5, but showing the mean GWL value for which the regional signal emerges consistently ( $^{\circ}\text{C}$ ). White cells indicate no emergence, as obtained from the RCP8.5 scenario for the twenty-first century



while the difference between scenarios varies from 1.2% (CMIP5) to 0.7% (CORDEX). Our results are consistent with the conclusions obtained by Ishizaki et al. (2012) -i.e. the emission scenario has small but higher influence in middle and high latitudes of the Northern Hemisphere-.

Our study demonstrates that CMIP5 and CORDEX are fairly consistent to assess the regional response to global warming at the large-scale analyzed here. Regional models are expected to provide added value when considering climate at smaller scales and/or for extremes (Giorgi et al. 2016). Some of the inconsistencies found have been linked to inconsistencies between GCMs and nested RCMs that may be reduced in the upcoming CORDEX-CMIP6, currently under development. As an example, the use of evolving aerosols consistent with the driving GCM is strongly encouraged by the new CORDEX-CMIP6 experiment design. This will likely tend to align even further the large-scale regional responses of both initiatives.

**Supplementary Information** The online version contains supplementary material available at <https://doi.org/10.1007/s00382-023-06790-y>.

**Acknowledgements** We acknowledge the Earth System Grid Federation (ESGF) infrastructure, an international effort led by the U.S. Department of Energy's Program for Climate Model Diagnosis and Intercomparison, the European Network for Earth System Modelling and other partners in the Global Organisation for Earth System Science Portals (GO-ESSP). We thank the two anonymous reviewers, who contributed to improve the final version of this work with their comments and suggestions.

**Author contribution** The formal analysis was developed by JD-S. All authors contribute to the conceptualization and investigation. Visualization (figures) and software were prepared by JD-S and JF. Project administration was done by JMG. The original draft preparation of the paper was written by JD-S, JMG and JF. All authors contributed to write, revise and edit the final draft.

**Funding** Open Access funding provided thanks to the CRUE-CSIC agreement with Springer Nature. This work is part of project ATLAS (PID2019-111481RB-I00) funded by MCIN/AEI/10.13039/501100011033. JF and ASC acknowledge support from project CORDyS (PID2020-116595RB-I00) funded by MCIN/AEI/10.13039/501100011033. ASC acknowledges project IS-ENES3 which is funded by the European Union's Horizon 2020 research and innovation programme under grant agreement No 824084.

**Data availability** The dataset used in the present study is available at the IPCC-WG1 Atlas repository (Iturbide et al. 2021, 2022).

**Code availability** The code (jupyter notebook in python programming language) used to generate key figures and the GWL plots for all the reference regions are available on GitHub ([https://github.com/Santa-nderMetGroup/2022\\_Diez-Sierra\\_GWLs](https://github.com/Santa-nderMetGroup/2022_Diez-Sierra_GWLs)) and Zenodo (Díez-Sierra et al. 2023).

## Declarations

**Conflict of interest** The authors declare that they have no conflict of interest.

**Open Access** This article is licensed under a Creative Commons Attribution 4.0 International License, which permits use, sharing, adaptation, distribution and reproduction in any medium or format, as long as you give appropriate credit to the original author(s) and the source, provide a link to the Creative Commons licence, and indicate if changes were made. The images or other third party material in this article are included in the article's Creative Commons licence, unless indicated otherwise in a credit line to the material. If material is not included in the article's Creative Commons licence and your intended use is not permitted by statutory regulation or exceeds the permitted use, you will need to obtain permission directly from the copyright holder. To view a copy of this licence, visit <http://creativecommons.org/licenses/by/4.0/>.

## References

- Boé J, Somot S, Corre L, Nabat P (2020) Large discrepancies in summer climate change over Europe as projected by global and regional climate models: causes and consequences. *Clim Dyn* 54:2981–3002. <https://doi.org/10.1007/s00382-020-05153-1>
- Ciarlo JM, Coppola E, Fantini A, Giorgi F, Gao X, Tong Y, Glazer RH, Torres Alavez JA, Sines T, Pichelli E, Raffaele F, Das S, Bukovsky M, Ashfaq M, Im E-S, Nguyen-Xuan T, Teichmann C, Remedio A, Remke T, Bülow K, Weber T, Bunte-meyer L, Sieck K, Rechid D, Jacob D (2021) A new spatially distributed added value index for regional climate models: the EURO-CORDEX and the CORDEX-CORE highest resolution ensembles. *Clim. Dyn.* 57:1403–1424. <https://doi.org/10.1007/s00382-020-05400-5>
- Déqué M, Calmanti S, Christensen OB, Dell'Aquila A, Maule CF, Haensler A, Nikulin G, Teichmann C (2017) A multi-model climate response over tropical Africa at +2°C. *Clim. Serv.* 7:87–95. <https://doi.org/10.1016/j.cliser.2016.06.002>
- Díez-Sierra J, Iturbide M, Gutiérrez JM, Fernández J, Milovac J, Cofiño AS, Cimadevilla E, Nikulin G, Levavasseur G, Kjellström E, Bülow K, Horányi A, Brookshaw A, García-Díez M, Pérez A, Baño-Medina J, Ahrens B, Alias A, Ashfaq M, Bukovsky M, Buonomo E, Caluwaerts S, Chou SC, Christensen OB, Ciarlo JM, Coppola E, Corre L, Demory M-E, Djurdjevic V, Evans JP, Fealy R, Feldmann H, Jacob D, Jayanarayanan S, Katzfey J, Keuler K, Kittel C, Kurnaz ML, Laprise R, Lionello P, McGinnis S, Mercogliano P, Nabat P, Önlü B, Öztürk T, Panitz H-J, Paquin D, Pieczka I, Raffaele F, Remedio AR, Scinocca J, Sevault F, Somot S, Steger C, Tangang F, Teichmann C, Termonia P, Thatcher M, Torma C, van Meijgaard E, Vautard R, Warrach-Sagi K, Winger K, Zittis G (2022) The worldwide C3S CORDEX grand ensemble: A major contribution to assess regional climate change in the IPCC AR6 Atlas. *Bull Am Meteorol Soc.* <https://doi.org/10.1175/BAMS-D-22-0111.1>
- Díez-Sierra J, Iturbide M, Fernández J, Gutiérrez JM, Milovac J, Cofiño AS (2023) Repository supporting the article—consistency of the regional response to global warming levels from CMIP5 and CORDEX projections- (v2.0.0). Zenodo. <https://doi.org/10.5281/zenodo.7736850>
- Doblas-Reyes FJ, Sörensson AA, Almazroui M, Dosio A, Gutowski WJ, Haarsma R, Hamdi R, Hewitson B, Kwon W-T, Lamptey BL, Maraun D, Stephenson TS, Takayabu I, Terray L, Turner A, Zuo Z (2021) Linking global to regional climate change, in: climate change 2021: the physical science basis. In: Masson-Delmotte V, Zhai P, Pirani A, Connors SL, Péan C, Berger S, Caud N, Chen Y, Goldfarb L, Gomis MI, Huang M, Leitzell K, Lonnoy E, Matthews JBR, Maycock TK, Waterfield T, Yelekçi O, Yu R, Zhou B (eds) Contribution of working group I to the sixth assessment report of the intergovernmental panel on climate change. Cambridge University Press, Cambridge



- Dosio A, Jones RG, Jack C et al (2019) What can we know about future precipitation in Africa? Robustness, significance and added value of projections from a large ensemble of regional climate models. *Clim Dyn* 53:5833–5858. <https://doi.org/10.1007/s00382-019-04900-3>
- Eyring V, Bony S, Meehl GA, Senior CA, Stevens B, Stouffer RJ, Taylor KE (2016) Overview of the coupled model intercomparison project phase 6 (CMIP6) experimental design and organization. *Geosci Model Dev* 9:1937–1958. <https://doi.org/10.5194/gmd-9-1937-2016>
- Falco M, Carril AF, Menéndez CG, Zaninelli PG, Li LZ (2019) Assessment of CORDEX simulations over South America: added value on seasonal climatology and resolution considerations. *Clim Dyn* 52:4771–4786. <https://doi.org/10.1007/s00382-018-4412-z>
- Giorgi F, Gutowski WJ (2015) Regional dynamical downscaling and the CORDEX initiative. *Annu Rev Environ Resour* 40:467–490. <https://doi.org/10.1146/annurev-environ-102014-021217>
- Giorgi F et al (2022) The CORDEX-CORE EXP-I initiative: description and highlight results from the initial analysis. *Bull Amer Meteor Soc* 103:E293–E310. <https://doi.org/10.1175/BAMS-D-21-0119.1>
- Giorgi F, Torma C, Coppola E et al (2016) Enhanced summer convective rainfall at Alpine high elevations in response to climate warming. *Nature Geosci* 9:584–589. <https://doi.org/10.1038/ngeo2761>
- Gosse H, Kay JE, Armour KC, Bodas-Salcedo A, Chepfer H, Docquier D, Jonko A, Kushner PJ, Lecomte O, Massonnet F, Park H-S, Pithan F, Svensson G, Vancoppenolle M (2018) Quantifying climate feedbacks in polar regions. *Nat Commun* 9:1919. <https://doi.org/10.1038/s41467-018-04173-0>
- Gutiérrez JM, Jones RG, Narisma GT, Alves LM, Amjad M, Gorodetskaya IV, Grose M, Klutse NAB, Krakovska S, Li J, Martínez-Castro D, Mearns LO, Mernild SH, Ngo-Duc T, van den Hurk B, Yoon J-H (2021) Atlas. In: Masson-Delmotte V, Zhai P, Pirani A, Connors SL, Péan C, Berger S, Caud N, Chen Y, Goldfarb L, Gomis MI, Huang M, Leitzell K, Lonnoy E, Matthews JBR, Maycock TK, Waterfield T, Yelekçi O, Yu R, Zhou B (eds) *Climate change 2021: the physical science basis contribution of working group I to the sixth assessment report of the intergovernmental panel on climate change*. Cambridge University Press, Cambridge, pp 1927–2058. <https://doi.org/10.1017/9781009157896.021>
- Gutowski WJ Jr, Giorgi F, Timbal B, Frigon A, Jacob D, Kang H-S, Raghavan K, Lee B, Lennard C, Nikulin G, O'Rourke E, Rixen M, Solman S, Stephenson T, Tangang F (2016) WCRP COordinated Regional Downscaling Experiment (CORDEX): a diagnostic MIP for CMIP6. *Geosci Model Dev* 9:4087–4095. <https://doi.org/10.5194/gmd-9-4087-2016>
- Gutowski WJ, Ullrich PA, Hall A, Leung LR, O'Brien TA, Patricia CM, Arritt RW, Bukovsky MS, Calvin KV, Feng Z, Jones AD, Kooperman GJ, Monier E, Pritchard MS, Pryor SC, Qian Y, Rhoades AM, Roberts AF, Sakaguchi K, Urban N, Zarzycki C (2020) The ongoing need for high-resolution regional climate models: process understanding and stakeholder information. *Bull Am Meteorol Soc* 101:E664–E683. <https://doi.org/10.1175/BAMS-D-19-0113.1>
- Hohenegger C, Brockhaus P, Bretherton CS, Schär C (2009) The soil moisture-precipitation feedback in simulations with explicit and parameterized convection. *J Clim* 22:5003–5020. <https://doi.org/10.1175/2009JCLI2604.1>
- Iles CE, Vautard R, Strachan J, Joussaume S, Eggen BR, Hewitt CD (2020) The benefits of increasing resolution in global and regional climate simulations for European climate extremes. *Geosci Model Dev* 13:5583–5607. <https://doi.org/10.5194/gmd-13-5583-2020>
- IPCC (2021a) *Climate change 2021: the physical science basis*. In: Masson-Delmotte V, Zhai P, Pirani A, Connors SL, Péan C, Berger S, Caud N, Chen Y, Goldfarb L, Gomis MI, Huang M, Leitzell K, Lonnoy E, Matthews JBR, Maycock TK, Waterfield T, Yelekçi O, Yu R, Zhou B (eds) *Contribution of working group I to the sixth assessment report of the intergovernmental panel on climate change*. Cambridge University Press, Cambridge
- IPCC (2021b) Annex II: models. In: Masson-Delmotte V et al (eds) *Climate change 2021: the physical science basis*. Cambridge University Press, Cambridge, pp 2087–2138. <https://doi.org/10.1017/9781009157896.016>
- IPCC (2022) *Climate Change 2022: Impacts, Adaptation, and Vulnerability*. In: Pörtner H-O, Roberts DC, Tignor M, Poloczanska ES, Mintenbeck K, Alegría A, Craig M, Langsdorf S, Lösschke S, Möller V, Okem A, Rama B (eds) *Contribution of working group II to the sixth assessment report of the intergovernmental panel on climate change*. Cambridge University Press, Cambridge
- Ishizaki Y, Shiogama H, Emori S, Yokohata T, Nozawa T, Ogura T, Abe M, Yoshimori M, Takahashi K (2012) Temperature scaling pattern dependence on representative concentration pathway emission scenarios: a letter. *Clim Change* 112(2):535–546. <https://doi.org/10.1007/s10584-012-0430-8>
- Iturbide M, Gutiérrez JM, Alves LM, Bedia J, Cerezo-Mota R, Cimaedevilla E, Cofiño AS, Di Luca A, Faria SH, Gorodetskaya IV, Hauser M, Herrera S, Hennessy K, Hewitt HT, Jones RG, Krakovska S, Manzanar R, Martínez-Castro D, Narisma GT, Nurhati IS, Pinto I, Seneviratne SI, van den Hurk B, Vera CS (2020) An update of IPCC climate reference regions for subcontinental analysis of climate model data: definition and aggregated datasets. *Earth Syst Sci Data* 12:2959–2970. <https://doi.org/10.5194/essd-12-2959-2020>
- Iturbide M, Fernández J, Gutiérrez JM, Bedia J, Cimaedevilla E, Díez-Sierra J, Manzanar R, Casanueva A, Baño-Medina J, Milovac J, Herrera S, Cofiño AS, San Martín D, García-Díez M, Hauser M, Huard D, Yelekçi Ö (2021) Repository Supporting the Implementation of FAIR Principles in the IPCC-WGI Atlas. Zenodo. <https://doi.org/10.5281/zenodo.5171760>
- Iturbide M, Fernández J, Gutiérrez JM, Pirani A, Huard D, Al Khouradje A, Baño-Medina J, Bedia J, Casanueva A, Cimaedevilla E, Cofiño AS, De Felice M, Díez-Sierra J, García-Díez M, Goldie J, Herrera DA, Herrera S, Manzanar R, Milovac J, Radhakrishnan A, San-Martín D, Spinuso A, Thyng KM, Trenham C, Yelekçi Ö (2022) Implementation of FAIR principles in the IPCC: the WGI AR6 Atlas repository. *Sci Data* 9:629. <https://doi.org/10.1038/s41597-022-01739-y>
- Jacob D, Teichmann C, Sobolowski S, Katragkou E, Anders I, Belda M, Benestad R, Boberg F, Buonomo E, Cardoso RM, Casanueva A, Christensen OB, Christensen JH, Coppola E, De Cruz L, Davin EL, Dobler A, Domínguez M, Fealy R, Fernandez J, Gaertner MA, García-Díez M, Giorgi F, Gobiet A, Goergen K, Gómez-Navarro JJ, Alemán JGG, Gutiérrez C, Gutiérrez JM, Güttler I, Haensler A, Halenka T, Jerez S, Jiménez-Guerrero P, Jones RG, Keuler K, Kjellström E, Knist S, Kotlarski S, Maraun D, van Meijgaard E, Mercogliano P, Montávez JP, Navarra A, Nikulin G, de Noblet-Ducoudré N, Panitz H-J, Pfeifer S, Piazza M, Pichelli E, Pietikäinen J-P, Prein AF, Preuschmann S, Rechid D, Rockel B, Romera R, Sánchez E, Sieck K, Soares PMM, Somot S, Srnc L, Sørland SL, Termonia P, Truhetz H, Vautard R, Warrach-Sagi K, Wulfmeyer V (2020) Regional climate downscaling over Europe: perspectives from the EURO-CORDEX community. *Rev Environ Change* 20:51. <https://doi.org/10.1007/s10113-020-01606-9>
- Kirchmeier-Young MC, Wan H, Zhang X, Seneviratne SI (2019) Importance of framing for extreme event attribution: the role of spatial and temporal scales. *Earth's Future* 7:1192–1204. <https://doi.org/10.1029/2019EF001253>
- Liang Y-C, Polvani LM, Mitevski I (2022) Arctic amplification, and its seasonal migration, over a wide range of abrupt CO<sub>2</sub> forcing. *Npj Clim Atmos Sci* 5:1–9. <https://doi.org/10.1038/s41612-022-00228-8>

- Matte D, Larsen MAD, Christensen OB, Christensen JH (2019) Robustness and scalability of regional climate projections over Europe. *Front Environ Sci*. <https://doi.org/10.3389/fenvs.2018.00163>
- Maule CF, Mendlik T, Christensen OB (2017) The effect of the pathway to a two degrees warmer world on the regional temperature change of Europe. *Clim Serv* 7:3–11. <https://doi.org/10.1016/j.cliser.2016.07.002>
- Müller OV, Vidale PL, Vanni  re B, Schiemann R, Senan R, Haarsma RJ, Jungclaus JH (2021) Land-atmosphere coupling sensitivity to GCMs resolution: a multimodel assessment of local and remote processes in the sahel hot spot. *J Clim* 34:967–985. <https://doi.org/10.1175/JCLI-D-20-0303.1>
- Nikulin G, Lennard C, Dosio A, Kjellstr  m E, Chen Y, H  nsler A, Kupiainen M, Laprise R, Mariotti L, Maule CF, van Meijgaard E, Panitz H-J, Scinocca JF, Somot S (2018) The effects of 1.5 and 2 degrees of global warming on Africa in the CORDEX ensemble. *Environ Res Lett*. 13:065003. <https://doi.org/10.1088/1748-9326/aab1b1>
- Pendergrass AG, Lehner F, Sanderson BM, Xu Y (2015) Does extreme precipitation intensity depend on the emissions scenario? *Geophys Res Lett* 42:8767–8774. <https://doi.org/10.1002/2015GL065854>
- Schwingshackl C, Davin EL, Hirschi M, S  rland SL, Wartenburger R, Seneviratne SI (2019) Regional climate model projections underestimate future warming due to missing plant physiological CO2 response. *Environ Res Lett*. <https://doi.org/10.1088/1748-9326/ab4949>
- Seneviratne SI, Hauser M (2020) Regional climate sensitivity of climate extremes in CMIP6 versus CMIP5 multimodel ensembles. *Earths Future*. 8:e2019EF001474. <https://doi.org/10.1029/2019E001474>
- Seneviratne SI, L  thi D, Litschi M, Sch  r C (2006) Land–atmosphere coupling and climate change in Europe. *Nature* 443:205–209. <https://doi.org/10.1038/nature05095>
- Seneviratne SI, Donat MG, Pitman AJ, Knutti R, Wilby RL (2016) Allowable CO2 emissions based on regional and impact-related climate targets. *Nature* 529:477–483. <https://doi.org/10.1038/nature16542>
- Seneviratne SI, Zhang X, Adnan M, Badi W, Luca AD, Ghosh S, Iskandar I, Kossin J, Lewis S, Otto F, Pinto I, Satoh M, Vicente-Serrano SM, Wehner M, Zhou B (2021) Weather and climate extreme events in a changing climate. In: Masson-Delmotte V, Zhai P, Pirani A, Connors SL, P  an C, Berger S, Caud N, Chen Y, Goldfarb L, Gomis MI, Huang M, Leitzell K, Lonnoy E, Matthews JBR, Maycock TK, Waterfield T, Yelek  i O, Yu R, Zhou B (eds) *Climate change 2021: the physical science basis. Contribution of working group I to the sixth assessment report of the intergovernmental panel on climate change*. Cambridge University Press, Cambridge, pp 1513–1766. <https://doi.org/10.1017/9781009157896.013>
- Taranu IS, Somot S, Alias A, Bo   J, Delire C (2022) Mechanisms behind large-scale inconsistencies between regional and global climate model-based projections over Europe. *Clim Dyn*. <https://doi.org/10.1007/s00382-022-06540-6>
- Taylor KE, Stouffer RJ, Meehl GA (2011) An overview of CMIP5 and the experiment design. *Bull Am Meteorol Soc* 93:485–498. <https://doi.org/10.1175/BAMS-D-11-00094.1>
- Teichmann C, Jacob D, Remedio AR, Remke T, Bunt  meyer L, Hoffmann P, Kriegsmann A, Lierhammer L, B  low K, Weber T, Sieck K, Rechid D, Langendijk GS, Coppola E, Giorgi F, Ciarlo JM, Raffaele F, Giuliani G, Xuejie G, Sines TR, Torres-Alavez JA, Das S, Di Sante F, Pichelli E, Glazer R, Ashfaq M, Bukovsky M, Im E-S (2021) Assessing mean climate change signals in the global CORDEX-CORE ensemble. *Clim Dyn*. 57:1269–1292. <https://doi.org/10.1007/s00382-020-05494-x>
- The Paris agreement, publication, UNFCCC (2016) <https://unfccc.int/documents/184656>. Accessed 15 July 22.
- Wartenburger R, Hirschi M, Donat MG, Greve P, Pitman AJ, Seneviratne SI (2017) Changes in regional climate extremes as a function of global mean temperature: an interactive plotting framework. *Geosci Model Dev* 10:3609–3634. <https://doi.org/10.5194/gmd-10-3609-2017>

**Publisher's Note** Springer Nature remains neutral with regard to jurisdictional claims in published maps and institutional affiliations.